行政院國家科學委員會專題研究計畫 成果報告

新穎 BiTe(Sb, Se)基熱電薄膜:三維可調控高方向性奈米結構、金屬奈米粒子介面修飾與高效能薄膜型熱電轉換元件 研究成果報告(精簡版)

計 畫 主 持 人 : 陳軍華

計畫參與人員 : 碩士班研究生-兼任助理人員:沈智仁
　　　　　　　　碩士班研究生-兼任助理人員:柯克憲
　　　　　　　　博士班研究生-兼任助理人員:張修誠
　　　　　　　　博士班研究生-兼任助理人員:楊景筌

報 告 附 件 : 出席國際會議研究心得報告及發表論文

公 開 資 訊 : 本計畫可公開查詢

中 華 民 國 100 年 11 月 01 日

中文摘要： 奈米結構熱電材料中，維度和尺寸、選擇性方向、幾何形貌及其組裝後的規則性往往扮演非常關鍵的角色。本研究成功開發出單一步驟、大面積、不需催化與模板的脈衝雷射沉積 (pulsed laser deposition, PLD)技術，可於二氧化矽/矽 (SiO2/Si)基板上，透過物理方式自組裝形成垂直排列(well-aligned)的碲化鉍(Bi2Te3)的奈米結構。經由精確的參數控制可得到四種重要的 Bi2Te3 自組裝結構，例如：零維奈米粒子 (0-D nanoparticles)、一維奈米柱(1-D nanorods)、二維奈米薄片(2-D nanoflakes)及三維奈米峽谷(3-D nanocanyons)，其所對應之優選方向分別為(006)、(015)、(110)和(006)。另外，我們提出奈米粒子輔助晶體成長機制，氣態電漿物質會因高背景壓力而凝結沉積於基板上，再藉由基板加熱造成奈米粒子內部的原子擴散及再重組形成一系列垂直排列之奈米結構。相對於雜亂排列之 Bi2Te3 奈米結構，垂直排列的零維至三維 Bi2Te3 奈米結構皆在室溫下展現較高之功率因子，其主要原因來自於內部電阻降低。研究結果證實精確控制奈米結構的排列對增進熱電性質是一種有效的策略，對於往後改良及設計更進階的熱電材料而言，具有極高參考價值。

英文摘要： The dimension and size of the building blocks as well as the preferential orientation, geometry and regularity of their assemblies are the most important key factors for fabricating thermoelectric materials with a high figure-of- merit (ZT) which is governed by the efficiencies in transporting electrical and thermal energies along the measurement direction. A one-step and large-area growth approach has been successfully developed employing pulsed laser deposition (PLD) for producing physically self-assembled and well-aligned Bi2Te3 nano- structures on SiO2/Si substrates without pre-built templates or catalysts. The precisely parameter controlled growth provides four highly reproducible and significant Bi2Te3 assemblies, comprising 0-dimensional (0-D) nanoparticles, 1-D nanorods, 2-D nanoflakes, and 3-D nano- canyons, respectively exhibiting an overall (006), (015), (110), and (006) preferential orientation normal to the substrate surface. The nanoparticle assisted crystal growth is proposed, mainly involving the condensation of the plasma species in the gas phase at higher ambient pressures and the following diffusion and reorganization of the

deposited nanoparticle atoms on the substrates. The well-aligned 0-D to 3-D Bi2Te3 nano- structures show more excellent in-plane power factors than most of the randomly aligned Bi2Te3 nanostructures at room temperature mainly due to significantly reducing inter resistance. The thermoelectric properties of these well-aligned Bi2Te3 nanostructures are comparable to any other intrinsic Bi2Te3 nano- structures that have ever been reported. The present data are valuable for further improving and designing advanced thermoelectric materials and confirm that precise control of nanostructural aggregation is an effective strategy for enhancing the thermo -electric performance.

新穎 BiTe (Sb, Se)基熱電薄膜：三維可調控高方向性奈米結構、金屬奈米粒子介面修飾與高效能薄膜型熱電轉換元件
Novel Sb/Se doped Bi-Te based thermoelectric thin films: three-dimensional control of highly oriented nano-structures, metallic nanoparticle modified interfaces and high-performance thin-film thermoelectric conversion devices

Abstract

The dimension and size of the building blocks as well as the preferential orientation, geometry and regularity of their assemblies are the most important key factors for fabricating thermoelectric materials with a high figure-of-merit (ZT) which is governed by the efficiencies in transporting electrical and thermal energies along the measurement direction. A one-step and large-area growth approach has been successfully developed employing pulsed laser deposition (PLD) for producing physically self-assembled and well-aligned Bi_2Te_3 nano-structures on SiO_2/Si substrates without pre-built templates or catalysts. The precisely parameter controlled growth provides four highly reproducible and significant Bi_2Te_3 assemblies, comprising 0-dimensional (0-D) nanoparticles, 1-D nanorods, 2-D nanoflakes, and 3-D nano-canyons, respectively exhibiting an overall (006), (015), (110), and (006) preferential orientation normal to the substrate surface. The nanoparticle assisted crystal growth is proposed, mainly involving the condensation of the plasma species in the gas phase at higher ambient pressures and the following diffusion and reorganization of the deposited nanoparticle atoms on the substrates. The well-aligned 0-D to 3-D Bi_2Te_3 nano-structures show more excellent in-plane power factors than most of the randomly aligned Bi_2Te_3 nanostructures at room temperature mainly due to significantly reducing inter resistance. The thermoelectric properties of these well-aligned Bi_2Te_3 nanostructures are comparable to any other intrinsic Bi_2Te_3 nano- structures that have ever been reported. The present data are valuable for further improving and designing advanced thermoelectric materials and confirm that precise control of nanostructural aggregation is an effective strategy for enhancing the thermo-electric performance.

Keywords: thermoelectric; PLD; Bi_2Te_3

摘要

奈米結構熱電材料中，維度和尺寸、選擇性方向、幾何形貌及其組裝後的規則性往往扮演非常關鍵的角色。本研究成功開發出單一步驟、大面積、不需催化與模板的脈衝雷射沉積(pulsed laser deposition, PLD)技術，可於二氧化矽/矽(SiO_2/Si)基板上，透過物理方式自組裝形成垂直排列(well-aligned)的碲化鉍(Bi_2Te_3)的奈米結構。經由精確的參數控制可得到四種重要的 Bi_2Te_3 自組裝結構，例如：零維奈米粒子(0-D nanoparticles)、一維奈米柱(1-D nanorods)、二維奈米薄片(2-D nanoflakes)及三維奈米峽谷(3-D nanocanyons)，其所對應之優選方向分別為(006)、(015)、(110)和(006)。另外，我們提出奈米粒子輔助晶體成長機制，氣態電漿物質會因高背景壓力而凝結沉積於基板上，再藉由基板加熱造成奈米粒子內部的原子擴散及再重組形成一系列垂直排列之奈米結構。相對於雜亂排列之 Bi_2Te_3 奈米結構，垂直排列的零維至三維 Bi_2Te_3 奈米結構皆在室溫下展現較高之功率因子，其主要原因來自於內部電阻降低。研究結果證實精確控制奈米結

構的排列對增進熱電性質是一種有效的策略，對於往後改良及設計更進階的熱電材料而言，具有極高參考價值。

Introduction

Nanostructuring has been widely accepted as one of the most effective strategies for significantly increasing the thermoelectric figure of merit $ZT=\sigma S^2 T \kappa^{-1}$ where σ is the electrical conductivity, S is the Seebeck coefficient, T is the absolute temperature, and κ is the thermal conductivity.[1-3] The theoretical studies of Bi_2Te_3 have obviously predicted the importance of controlling size and dimension.[4,5] For instance, the ZT for a 2-D quantum well (3.8 Å thickness) and a 1-D quantum wire (squared cross section of 5 Å width) is about 16 and 27 times higher, respectively, comparing with that for bulk (ZT~0.52). Experimental data for single quantum crystal is extremely lacking due to the technological difficulties of the thermoelectric measurements of such small crystals. Balandin et al. experimentally proved that an about 30–40% enhancement in ZT for an ultra-thin quasi-2D Bi_2Te_3 crystal was mainly contributed from the great drop of the thermal conductivity from 0.5–0.6 $Wm^{-1}K^{-1}$ (bulk) to 0.1–0.3 $Wm^{-1}K^{-1}$ in the cross plane direction at room temperature.[6] The presence of boundaries or interfaces accompanying with the decreased size or dimension is considered to be the key to effectively inhibit not only the thermal conductivity but usually also the electrical conductivity. A remarkable electrical conductivity thus is helpful to approach a high ZT for quantum crystals because of the competition relation between these two parameters as described above. It has been reported that a single Bi_2Te_3 nanowire (77 nm diameter) can present a high electrical conductivity (860 Scm^{-1})[7] which is at same order of magnitude compared to that obtained from bulk (900 Scm^{-1})[8]. In this case, in comparison with Bi_2Te_3 bulk, a higher ZT may be found owing to an expected lower thermal conductivity.

Even though individual Bi_2Te_3 quantum crystals have experimentally and theoretically demonstrated excellent thermoelectric performance, there still exist many technological problems in fabrication as well as characterization for further applications. Assembling of the quantum crystals, i.e. a film or bulk with nanostructures, thus becomes a much more feasible way for fundamental studies and practical applications. It is believed that orderly assembling of the nanostructures may be an advanced strategy for novel thermoelectric materials and devices since the electrical and thermal energy can be effectively transport in the orderly structures[9,10]. For practical example, the breakthrough of the Bi_2Te_3/Sb_2Te_3 superlattices (ZT~2.4) were considered as the results of an effective increase of the state density near the Fermi level and the phonon transport resistance contributed by the quantum confinement effect[11]. Due to these exhilarating investigations, many efforts have focused on the preparation of assembles of Bi_2Te_3 nanocrystals with various morphologies, e.g. nanoparticles[12-14], nano-wires[9,15], nanorods[10,16], and nanoplates[17,18], to introduce the spatial confinement. However, till now, most cases of the nanocrystal assembles are randomly-aligned to substrates. It is hence not easy to obtain predicted significant thermoelectric properties. Well-aligned Bi_2Te_3 nanostructures prepared by template- or catalysis-free approaches were less reported. In addition, Bi_2Te_3 nanostructures with spatial confinements from 1-D to 3-D nanocrystals also have not been systematically fabricated and studied yet. These technological issues indeed need to be clarified for the further enhancement of thermoelectric materials.

In this work, we present an optimized one-step, large-area, noncatalystic and template-free growth approach to distinct Bi_2Te_3 nano-structures by pulsed laser deposition (PLD). By optimizing the substrate temperature and background atmosphere, four physically self-assembled and well-aligned Bi_2Te_3 nano-structured films respectively consisting of 0-D nanoparticles, 1-D nanorods, 2-D nanoflakes, and 3-D nanocanyons with specific preferential orientations normal to the insulated SiO_2/Si substrates were newly fabricated. Most

significantly, this is the first time that such many featured and well-aligned Bi_2Te_3 nanostructures have been fabricated and reproducible by single deposition process. Moreover, this approach not only provides controllable microstructures but also overcomes many technological issues, such as the pollution of the residual templates or catalysts and the oxidation of the formed nanostructures. In order to obtain reliable thermoelectric related data and to evident well-aligned nanostructures as an advanced strategy, the thermoelectric properties were confirmed with independent characterization equipments and methods. This paper is expected to provide a better comprehension of the relation between the in-plane thermoelectric properties and structural characteristics and to offer a promise for realizing high-ZT thermoelectric nanostructures.

Experimental

Nanostructure deposition: The Bi_2Te_3 powders were dry pressed into discs of 10 mm diameter and 2 mm thickness and were then annealed under hydrogen ambient at 20 torr at 300 °C for 10 h. In order to prevent the substrate effect on the following thermoelectric measurement, a SiO_2 layer with a thickness of 500 nm was thermally grown on Si substrates. The crystal structure and composition of the prepared targets for PLD were confirmed as those of the starting powders. A Q-switched Nd:YAG pulsed laser (Litron, LPY 664) with a focused laser fluence of about 8.3 J/cm^2 (355 nm wavelength, 10 ns pulse duration, 8 mm beam diameter and 5 Hz repetition rate) was kept for the deposition processes. The deposition chamber was evacuated to a base pressure of 5×10^{-6} torr and 99.999% purity Ar was then introduced for the pressure control at various substrate temperatures from 250 to 550 °C.

Structure analysis: The morphology, size, and composition of the well-aligned 0-D to 3-D Bi_2Te_3 nanocrystals were examined by field emission scanning electron microscopy (FE-SEM, JEOL JSM-6500) with energy disperse spectroscopy (EDS, Oxford). The orientation and crystallinity of these four Bi_2Te_3 nanostructures were determined by x-ray diffraction (XRD, Bruker AXS, D8 Discover)

with $CuK\alpha$ radiation (λ=1.54 Å) in θ-2θ configuration and transmission electron microscopy (TEM, JEOL JEM-2100 and JEM-3000F). The oxidation state of the Bi_2Te_3 nanostructures was characterized by x-ray photoelectron microscopy (XPS, Thermo VG 350).

Thermoelectric characterization: The current-voltage (I-V) curve and the electrical conductivity of the Bi_2Te_3 nanostructures were respectively measured from the two-probe (Keithley 2400) and four-probe methods (CMT SR2000N) with gold electrodes. The corresponding carrier concentration and mobility were examined with a Hall system (Accent HL5500). The cross section SEM images provided the accurate thicknesses needed. The Keithley 2400 was utilized to provide thermal energy on one side of the specimen, and a maximum temperature gradient of 16 °C was then created between two electrodes with an interval of 1.0 cm. The Seebeck voltage and temperature difference were recorded in-situ and plotted for obtaining the Seebeck coefficients.

Results and discussion

Figure 1 shows the cross section and top view SEM images of the nanoblock assembled Bi_2Te_3 films deposited at various substrate temperatures, revealing uniform featured nanocrystals which can be respectively identified as 0-D nanoparticles, 1-D nanorods, 2-D nano-flakes, and 3-D nanocanyons. The corresponding size distributions were statistically counted from the SEM images. The 0-D nanoparticles deposited at 300 °C were pretty dense with an average diameter of 19 nm (see Fig. 2(a)). The 1-D nanorods deposited at 250 °C were perpendicularly aligned to the substrates with a height of ~1400 nm and an average width of ~130 nm for the square-like cross section as can be seen in Fig. 2(b). Similarly, the 2-D nanoflakes formed at 500 °C were also aligned perpendicularly to the substrates (Fig. 1(c)). A special cross link between these nanoflakes can be clearly observed in Fig. 1(g). The mean width, thickness and height were 690, 56, and 1740 nm, respectively, as shown in Fig. 2(c). The 3-D nanocanyons which consist of layered structures deposited at 550 °C have a stacking height of
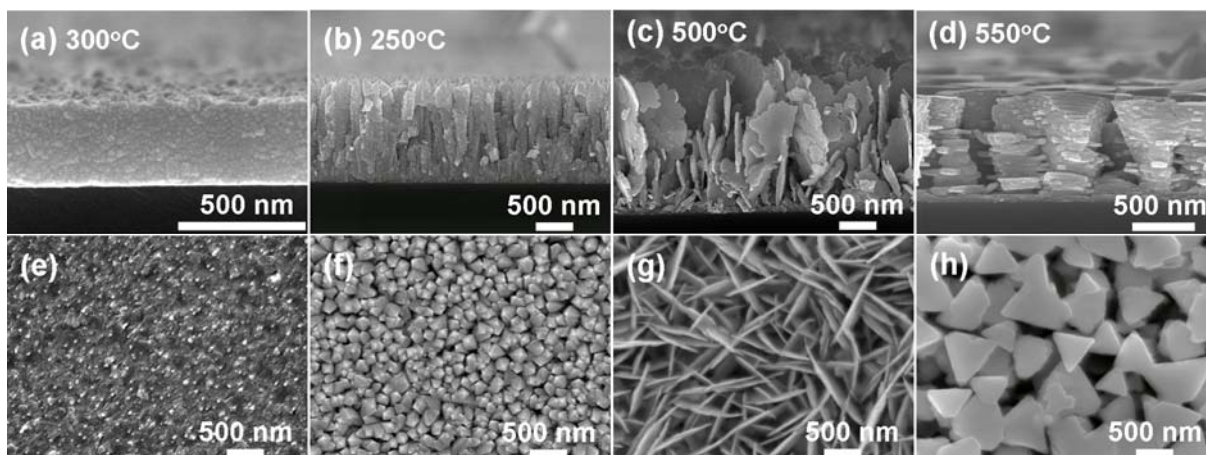
Fig. 1 The cross section SEM images of the (a) 0-D nanoparticles, (b) 1-D nanorods, (c) 2-D nanoflakes and (d) 3-D nanocanyons assembled Bi_2Te_3 nanostructures deposited at 300, 250, 500, and 550 ^oC for 3h, respectively. The corresponding top view SEM images are shown in (e), (f), (g) and (h).

~880 nm (Fig. 1(d)). The triangle-like top view (Fig. 1(h)) has an average width of ~440 nm (Fig. 2(d)).

According to the XRD patterns as shown in Fig. 3(a), all these four nanostructures can be mainly identified as the Bi_2Te_3 rhombohedral phase (JCPDS 89-4302) with respective out-of-plane preferential orientations. It is surprising that the recorded peaks for 0-D nanoparticles seem perfectly random, however, the relative high integrated intensity of the (006) peak indicating the occurrence of the anisotropic growth. For the well-aligned 1-D nanorods, the (015) direction clearly dominated the out-of-plane preferential growth. The only impurity peak found neighbor to Bi_2Te_3 (015) was identified as Te (101) (JCPDS 89-4899), which might originate from the wider spatial distribution of the Te plume than that of the Bi one because of the feasible volatile behavior of the Te element in PLD[19]. For the 2-D nanoflakes, the (110) peak is determined as the preferential orientation by numerical analysis with other peaks. In contrast to the (015) and (110) preferential orientation for the nanorods and nanoflakes, respectively, the 3-D nanocanyons display a strong c-axis preferential orientation, i.e. (006). The chemical composition and binding energy of these four nanostructures were evaluated by EDS and XPS, respectively. Four elements, Bi, Te, Si and O

can be clearly observed in the EDS spectra. The deviation of the Bi/Te composition (see Table 1) with the substrate temperatures is frequently observed in various deposition techniques. The binding energy of 157.2 eV and 162.5 eV shown in Fig. 3(b), and of 572.2 eV and 582.5 eV in Fig. 3(c) can be indexed as the $4f_{7/2}$ and $4f_{5/2}$ band for Bi^0, and $3d_{5/2}$ and $3d_{3/2}$ band for Te^0, respectively. The absence of the oxidation states for both Bi and Te is in agreement with
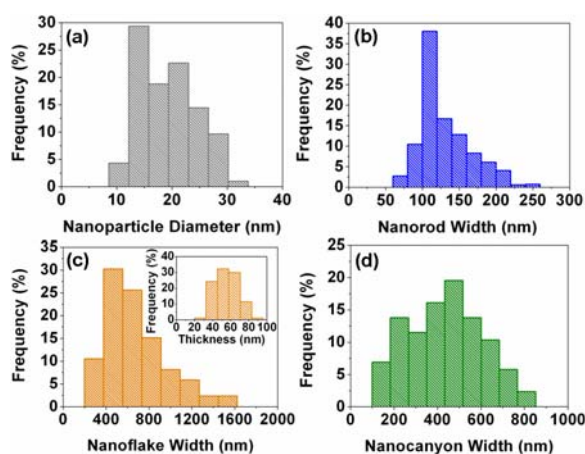
Fig. 2 The size distributions of (a) the diameter of the nanoparticles (cross section SEM image), (b) the width of the square-like cross section of the nanorods, (c) the width and thickness (inset) of the nanoflakes, and (d) the width of the nanocanyons. (b), (c), and (d) were obtained from the top view SEM images.
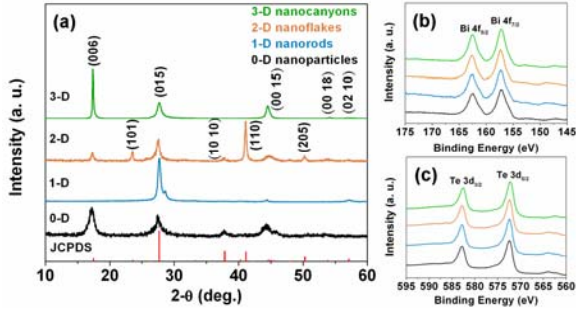
Fig. 3 (a) XRD patterns recorded for the well-aligned 0-D to 3-D Bi_2Te_3 nanostructures formed at various deposition temperatures. The indexed reflections correspond to the rhombohedral Bi_2Te_3 (JCPDS 89-4302). The corresponding XPS spectra of the (b) Bi 4f and (c) Te 3d state evidence the absence of oxidation states.

Table 1 The EDS chemical composi\tion of the well-aligned 0-D to 3-D Bi_2Te_3 nanostructures.

Composition	0-D nanoparticles	1-D nanorods	2-D nanoflakes	3-D nanocanyons
Bi (at%)	39.78	37.96	43.05	44.82
Te (at%)	60.22	62.04	56.95	55.18

the XRD observations and will be the merit for their electrical conductivity.

The cross section TEM images of the well-aligned 0-D to 3-D nanostructures are shown in Fig. 4(a)-(d), and the square marks the region for the selected-area electron diffraction (SAED) as displayed in Fig. 4(e)-(h). The slightly diffused SAED spots indicate that each morphological unit of the Bi_2Te_3 nanostructures excluding 0-D is not a perfect single crystal but is an ordered assembly of nanocrystals with slight misorientations. According to the mean size (see Fig. 2(a)), the region selected for SAED may contain only few 0-D nanoparticles. Thus, a clear ring pattern cannot be observed even though the stacks of the 0-D nanoparticles are quite random as mentioned in Fig. 3(a). As can be seen in Fig. 4(b), the head of the 1-D nanorods is tetrahedral-like and the clear diffused (015) spots shown in Fig. 4(f) is in agreement with the out-of-plane orientation determined by XRD. From Fig. 4(c), the triangle-like shape of one piece of the free-standing 2-D nanoflakes can be clearly seen and the Moiré fringes marked by the dash circle prove the existence of the small angle grain boundaries within the nanoflakes. In addition, the pair of (110) diffraction spots and the relative unobvious diffraction spots, (101), (015) and (205) appeared in Fig. 4(g) indicates the (110) out-of-plane preferential orientation. In the case of the 3-D nanocanyons, the Moiré fringes also can be observed in Fig. 4(d) and the corresponding slightly diffused SAED pattern (Fig. 4(h)) should originate from the minor stacking misorientations in both out-of-plane and in-plane directions.

Here we briefly summarize the structural investigations as plotted in Fig. 5 that the Bi_2Te_3 nanocrystals including 0-D nanoparticles, 1-D nanorods, 2-D nanoflakes, and 3-D nanocanyons were formed and well-aligned at 300, 250, 500, and 550 °C with an overall (006), (015), (110), and (006) preferential orientation, respectively. During the PLD process, the high-energy laser beams will lead various complicated physical and chemical phenomena which will greatly affect the film growth[20]. Thus, the variety of these distinct nanostructured films should result from not only the strong anisotropic growth behavior of Bi_2Te_3[21], but also the optimized deposition parameters.

In this work, all the thermoelectric properties were measured along the in-plane direction and shown in Table 2. Hall measurements confirmed that all the prepared nanostructures were electron-type carrier domination. The carrier concentration of the 0-D nanoparticles ($\sim 9\times 10^{19}$ cm^{-3}) is quite close to that of the 1-D nanorods and is higher than that of the 2-D nanoflakes and 3-D nanocanyons ($\sim 2\times 10^{19}$ cm^{-3}) since Te is volatile at higher deposition temperatures[19] (see Table 1). The carrier mobility measured from the 0-D to 3-D Bi_2Te_3 nanostructures is 14.8, 2.0, 31.9, and 19.5 cm^{2}V^{-1}s^{-1}, respectively. The I-V curve showed the excellent linearity over the entire range of applied voltages and indicated that the contacts are ohmic (see Fig. 6(a)). The slope of the four Bi_2Te_3 nanostructures yielded the resistance of 590, 790, 230, and 124 Ω, respectively. We also determined the electrical
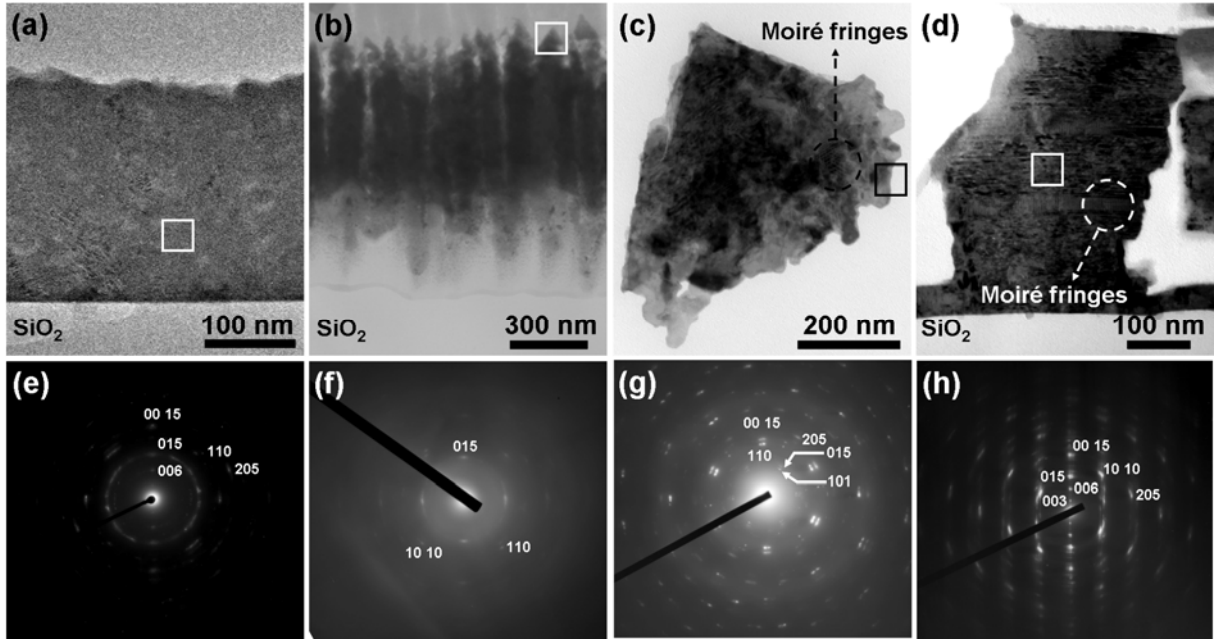
Fig. 4 The cross section TEM images of the (a) 0-D nanoparticles, (b) 1-D nanorods, (c) 2-D nanoflakes, and (d) 3-D nanocanyons. The corresponding SAED patterns taken from the squared region are shown in (e), (f), (g), and (h).

conductivity from the four-probe method is 230, 29, 78, and 70 Scm^{-1}, which is close to the result of the Hall measurement. The Seebeck coefficient (see Fig. 6(b)) for the 0-D to 3-D Bi_2Te_3 nanostructures exhibit similar levels with that for intrinsic Bi_2Te_3 bulk, which also confirm their n-type semiconductor behavior. Higher deposition temperatures (2-D and 3-D) seem important for obtaining of higher Seebeck coefficients where the averaged value is -91, -81, -132, and -143 μVK^{-1} for the 0-D to 3-D, respectively. However, the electrical conduc-tivity would be generally sacrificed with the Seebeck coefficient increasing due to the opposite tendency for these two parameters.

The in-plane power factor is 1.90, 0.19, 1.35, and 1.43 $Wcm^{-1}K^{-2}$ respectively for the 0-D to 3-D nanostructures as shown in Table 2. The present dry synthesis process is considered to provide clean and solid contacts between nanoparticles (see Fig. 3(b) and (c)). It is thus to achieve the relative high power factors. For instance, the present dense 0-D nanoparticle (~19 nm diameter) films exhibit about eight times higher in the electrical conductivity but an only ~40 % lower in the Seebeck coefficient comparing with the sintered pellets completely consisted with nanoparticles (~39 nm

diameter)[13]. In addition to the grain conductance, of course the particle size would also be an important issue. When the nanoparticle size of the pellets decreases to sub 10 nm,[12] a further
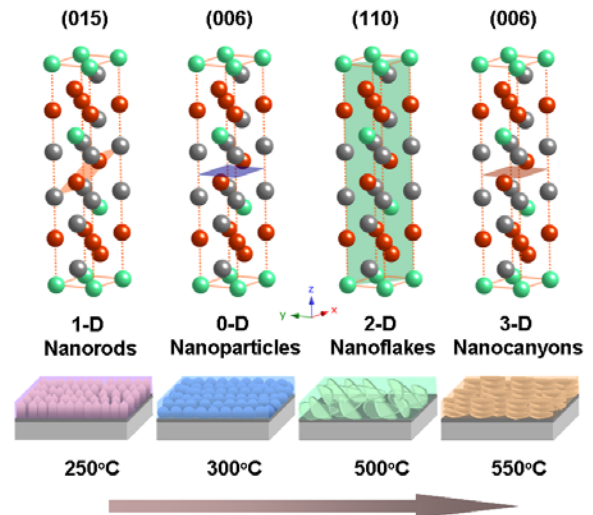
Fig. 5 Illustration of the preferential orientation, the dimension of the nanocrystals and the alignment with respect to the substrates under various deposition temperatures ranging from 250 to 550 °C. The gray, green, and red spheres represent the Bi, $Te^{(1)}$, and $Te^{(2)}$ atom positions, respectively.

6

enhancement in ZT was experimentally found that about three times increase in the electrical conductivity and an only ~11 VK^{-1} decrease in the Seebeck coefficient comparing with the present 0-D nanoparticle films. The decrease of the Seebeck coefficient with grain size have similar tendency as the theoretical prediction by Glatz and Beloborodov[22]. It is generally believed that the well alignment is of critical important for 1-D nanostructures to present distinct properties. The power factor of the well-aligned 1-D nanorods is significantly enhanced in comparison with that of the randomly-aligned quantum rods (~70 nm in diameter synthesized by chemical processes)[10]. Greatly improved electrical conductivity of the well-aligned 1-D nanorods would be the point as discussed in the 0-D nanoparticles. Similarly, Deng and Xiang also showed a competitive data measured from the Bi$_2$Te$_3$ quantum-wire arrays (prepared by vacuum deposition).[9] From the

SEM images (Fig. 1), the well-aligned 2-D nanoflakes exhibit much porous assembles than the 0-D and 1-D nanostructures. It is thus not expected to have an excellent electrical conductivity which is considered as the most critical parameter for most assembled nanostructures. But the well alignment is still helpful for the contribution of the electrical conductivity, comparing with the randomly-aligned nanoflakes[9] and the micro-spherical bouquet with 2-D nanoplates[17]. In contrast to the foregoing structures, the well-aligned 3-D nanocanyons have not been previously reported and showed an excellent power factor only inferior to 0-D nanoparticles. The relative high electrical conductivity is still the main reason. It is reasonable to believe that the air-filled interspaces between individual nanostructures will not remarkably inhibit the electron transport, but may be an effectively medium for resisting phonon transport[23].

Table 2 Room-temperature thermoelectric properties of the well-aligned 0-D to 3-D Bi$_2$Te$_3$ nanostructures.

Thermoelectric properties	0-D nanoparticles	1-D nanorods	2-D nanoflakes	3-D nanocanyons
Carrier concentration (10^{19} cm^{-3})	9.70	9.14	1.52	2.24
Carrier mobility (cm^{2}V^{-1}s^{-1})	14.8	2.0	31.9	19.5
Electrical conductivity (Scm^{-1})	230	29	78	70
Seebeck coefficient (μVK^{-1})	-91	-81	-132	-143
Power factor (μWcm^{-1}K^{-2})	1.90	0.19	1.35	1.43
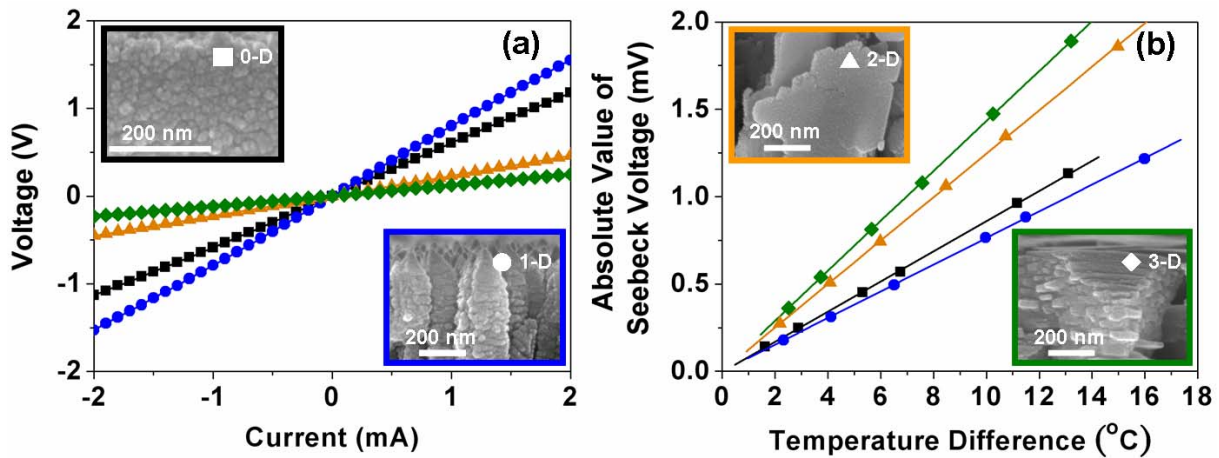
Fig. 6 (a) The I-V curve and (b) the Seebeck voltage plotted as a function of the temperature difference across the well-aligned 0-D to 3-D Bi$_2$Te$_3$ nanostructures. Insets are the corresponding cross section SEM images.

Conclusions

We have successfully demonstrated the systematic fabrication of physically self-assembled and well-aligned Bi_2Te_3 nanostructures on SiO_2/Si substrates without pre-built templates or catalysts by PLD at various substrate temperatures ranging from 250 to 550 ^{o}C. The building nanocrystals of the prepared Bi_2Te_3 nanostructures were clearly identified as the 0-D nanoparticles, 1-D nano- rods, 2-D nanoflakes, and 3-D nanocanyons and were found to be orderly-aligned on SiO_2/Si substrates with an overall (006), (015), (110), and (006) preferential orientation, respectively. The well-aligned 0-D to 3-D Bi_2Te_3 nanostructures show excellent in-plane power factor of 1.90, 0.19, 1.35, and 1.43 $Wcm^{-1}K^{-2}$, respectively. It is worth to notice that most of the randomly-aligned intrinsic Bi_2Te_3 nanostructured films generally present values smaller than 1 $W\ cm^{-1}K^{-2}$ at room temperature. The experimental evidence provided that the significant improvement in the power factor mainly originates from to the reduction of the inter resistance.

References

1. M. S. Dresselhaus, G. Chen, M. Y. Tang, R. Yang, H. Lee, D. Wang, Z. Ren, J. -P. Fleurial and P. Gogna, *Adv. Mater.*, 2007, **19**, 1043.
2. B. Poudel, Q. Hao, Y. Ma, Y. C. Lan, A. Minnich, B. Yu, X. Yan, D. Z. Wang, A. Muto, D. Vashaee, X. Y. Chen, J. M. Liu, M. S. Dresselhaus, G. Chen and Z. F. Ren, *Science*, 2008, **320**, 634.
3. B. C. Sales, *Science*, 2002, **295**, 1248.
4. L. D. Hicks and M. S. Dresselhaus, *Phys. Rev. B*, 1993, **47**, 12727.
5. L. D. Hicks and M. S. Dresselhaus, *Phys. Rev. B*, 1993, **47**, 16631.
6. D. Teweldebrhan, V. Goyal and A. A. Balandin, *Nano Lett.*, 2010, **10**, 1209.
7. J. Ham, W. Shim, D. H. Kim, S. Lee, J. Roh, S. W. Sohn, K. W. Oh, P. W. Voorhees and W. Lee, *Nano Lett.*, 2009, **9**, 2867.
8. D. M. Rowe, Thermoelectrics Handbook: Macro to Nano. CRC: 2005; pp 20-1-20-12.
9. Y. Deng, Y. Xiang and Y. Song, *Cryst. Growth Des.*, 2009, **9**, 3079.
10. A. Purkayastha, F. Lupo, S. Kim, T. Borca-Tasciuc and G. Ramanath, *Adv. Mater.*, 2006, **18**, 496.
11. R. Venkatasubramanian, E. Siivola, T. Colpitts and B. O'Quinn, *Nature*, 2001, **413**, 597.
12. M. Scheele, N. Oeschler, K. Meier, A. Kornowski, C. Klinke and H. Weller, *Adv. Funct. Mater.*, 2009, **19**, 3476.
13. M. R. Dirmyer, J. Martin, G. S. Nolas, A. Sen and J. V. Badding, *Small*, 2009, **5**, 933.
14. A. Purkayastha, S. Kim, D. D. Gandhi, P. G. Ganesan, T. Borca-Tasciuc and G. Ramanath, *Adv. Mater.*, 2006, **18**, 2958.
15. H. Yu, P. C. Gibbons and W. E. Buhro, *J. Mater. Chem.*, 2004, **14**, 595.
16. A. Purkayastha, Q. Yan, M. S. Raghuveer, D. D. Gandhi, H. Li, Z. W. Liu, R. V. Ramanujan, T. Borca-Tasciuc and G. Ramanath, *Adv. Mater.*, 2008, **20**, 2679.
17. T. Wang, R. Metha, C. Karthik, P. G. Ganesan, B. Singh, W. Jiang, N. Ravishankar, T. Borca-Tasciuc and G. Ramanath, *J. Phys. Chem. C*, 2010, **114**, 1796.
18. W. Lu, Y. Ding, Y. Chen, Z. L. Wang and J. Fang, *J. Am. Chem. Soc.*, 2005, **127**, 10112.
19. A. Bailini, F. Donati, M. Zamboni, V. Russo, M. Passoni, C. S. Casari, A. L. Bassi and C. E. Bottani, *Appl. Surf. Sci.*, 2007, **254**, 1249.
20. M. N. R. Ashfold, F. Claeyssens, G. M. Fuge and S. J. Henley, *Chem. Soc. Rev.*, 2004, **33**, 23.
21. W. Wang, J. Goebl, L. He, S. Aloni, Y. Hu, L. Zhen and Y. Yin, *J. Am. Chem. Soc.*, 2010, **132**, 17316.
22. A. Glatz and I. S. Beloborodov, *Phys. Rev. B*, 2009, **79**, 041404-8 (R).
23. Y. P. Mamunya, V. V. Davydenko, P. Pissis and E. V. Lebedev, *Eur. Polym. J.*, 2002, **38**, 1887.

Related Papers

H. C. Chang and C. H. Chen, "Self-assembled Bismuth Telluride Films with Well-Aligned Zero- to Three-Dimensional Nanoblocks for Thermoelectric Applications", *CrystEngComm* **2011**, *13*, 5956-5962.

Related Conferences

1. H. C. Chang, C. H. Chen*, and T. W. Chung, 'Deposition and In-Plane Thermoelectric Properties of Highly-Oriented Zero- to Three-Dimensional Bi_2Te_3 Nanostructures', 218th The Electrochemical Society (ECS) Meeting, Las Vegas, Nevada, Oct. 10-15, 2010.

2. H. C. Chang, and C. H. Chen*, "Well-aligned Bismuth Telluride Nanostructures by Pulsed Laser Deposition', International Conference on Materials for Advanced Technologies 2011 (ICMAT 2011), Singapore, June 26~July 1st, 2011.

國科會出國報告書

報告人姓名	陳軍華		職稱	助理教授
出國類別	□考察 □訪問 □進修 □研究 ■國際會議 □其他：＿＿＿			
會議/出國計畫名稱	International Conference on Materials for Advanced Technologies			
出國期間	自 100 年 6 月 26 日至 100 年 7 月 1 日		出國地點	新加坡
出國目的/發表論文題目	參加會議發表			

一、出國目的：

　　會議發表。

二、參加經過與心得：

　　本次出國參加 International Conference on Materials for Advanced Technologies (ICMAT)國際會議(6/26~7/1)，每二年於新加坡 SUNTEC 貿易展覽館召開，今年共分為 8 個主題(nanoscience and technology, energy and the environment, functional materials, bio/soft materials, imaging, crystal growth and crystal technology, interdisciplinary) ，共計 40 個 Symposium。本次主要在 nanoscience and technology 主題下 12 個 Symposium 中之 Symposium M "Nanonets and Nanomaterials for Energy Harnessing and Storage" 中進行發表。題目為 "Well-aligned Bismuth Telluride Nanostructures by Pulsed Laser Deposition"，為今年國科會專題研究計畫之重要產出。會議中所發表之內容，除了轉投會議集 "Nanoscience and Nanotechnology letters" 之外，其後更深入之研究成果，並已發表於知名結晶學國際期刊 CrystEngComm (IF: 4.0)。在此次能源相關之議題中，就熱電相關材料而言，會議中相關發表數量並不多，顯示現代熱電研究仍屬萌芽階段，但其必為太陽光電後，另一個最具潛力之綠色能源。而在此些少數熱電相關發表中發現，與本研究之薄膜熱電材料研發相異，多數研究乃屬材料應用，亦即利用目前眾所周知之熱電材料，進行各種熱電元件之設計，其中不乏相當值得參考之元件設計，對於未來本熱電材料研究之延伸，具有相當之參考價值。

除了熱電主題之外，金屬奈米粒子表面電漿共振(SPR)之研究亦為本次會議的一個重要獨立主題。在聆聽來自法國及美國各學者在 SPR 之報告後，對於 SPR 有了更深一層之應用理解。而理論計算在此領中扮演非常重要的角色，為了有效進行模擬計算，高速平行計算電腦(GPU)的建置成為必要之投資，此 GPU 電腦在材料科學上之應用尚屬初步之階段，值得國內學者注意。

　　綜觀來說，本會議參加人士領域相當廣泛，是材料直接相關之亞洲大型國際會議之一，參加國家及人數眾多，本系師生亦多人與會，會中與各國專家進行各種交流，除了提高個人研究之能見度外，並創造了許多後續研究合作的機會，並從各項發表最新研究內容中獲得許多創新之想法。

攜回資料名稱及內容
1. 會議手冊
2. 會議摘要
3. 會議議程表

國科會補助計畫衍生研發成果推廣資料表

日期:2011/11/01

國科會補助計畫	計畫名稱: 新穎BiTe(Sb,Se)基熱電薄膜：三維可調控高方向性奈米結構、金屬奈米粒子介面修飾與高效能薄膜型熱電轉換元件
	計畫主持人: 陳軍華
	計畫編號: 99-2221-E-009-041-　　　　　學門領域: 金屬

<div align="center">

無研發成果推廣資料

</div>

99 年度專題研究計畫研究成果彙整表

計畫主持人：陳軍華　　計畫編號：99-2221-E-009-041-

計畫名稱：新穎 BiTe(Sb,Se)基熱電薄膜：三維可調控高方向性奈米結構、金屬奈米粒子介面修飾與高效能薄膜型熱電轉換元件

<table>
<tr><td rowspan="2" colspan="2">成果項目</td><td colspan="3">量化</td><td rowspan="2">單位</td><td rowspan="2">備註（質化說明：如數個計畫共同成果、成果列為該期刊之封面故事...等）</td></tr>
<tr><td>實際已達成數（被接受或已發表）</td><td>預期總達成數(含實際已達成數)</td><td>本計畫實際貢獻百分比</td></tr>
<tr><td rowspan="16">國內</td><td rowspan="4">論文著作</td><td>期刊論文</td><td>0</td><td>0</td><td>100%</td><td rowspan="4">篇</td><td></td></tr>
<tr><td>研究報告/技術報告</td><td>0</td><td>0</td><td>100%</td><td></td></tr>
<tr><td>研討會論文</td><td>0</td><td>0</td><td>100%</td><td></td></tr>
<tr><td>專書</td><td>0</td><td>0</td><td>100%</td><td></td></tr>
<tr><td rowspan="2">專利</td><td>申請中件數</td><td>0</td><td>0</td><td>100%</td><td rowspan="2">件</td><td></td></tr>
<tr><td>已獲得件數</td><td>0</td><td>0</td><td>100%</td><td></td></tr>
<tr><td rowspan="2">技術移轉</td><td>件數</td><td>0</td><td>0</td><td>100%</td><td>件</td><td></td></tr>
<tr><td>權利金</td><td>0</td><td>0</td><td>100%</td><td>千元</td><td></td></tr>
<tr><td rowspan="4">參與計畫人力（本國籍）</td><td>碩士生</td><td>2</td><td>2</td><td>100%</td><td rowspan="4">人次</td><td></td></tr>
<tr><td>博士生</td><td>2</td><td>1</td><td>100%</td><td></td></tr>
<tr><td>博士後研究員</td><td>0</td><td>0</td><td>100%</td><td></td></tr>
<tr><td>專任助理</td><td>0</td><td>0</td><td>100%</td><td></td></tr>
<tr><td rowspan="16">國外</td><td rowspan="4">論文著作</td><td>期刊論文</td><td>1</td><td>1</td><td>100%</td><td rowspan="3">篇</td><td></td></tr>
<tr><td>研究報告/技術報告</td><td>1</td><td>1</td><td>100%</td><td></td></tr>
<tr><td>研討會論文</td><td>2</td><td>2</td><td>100%</td><td></td></tr>
<tr><td>專書</td><td>0</td><td>0</td><td>100%</td><td>章/本</td><td></td></tr>
<tr><td rowspan="2">專利</td><td>申請中件數</td><td>0</td><td>0</td><td>100%</td><td rowspan="2">件</td><td></td></tr>
<tr><td>已獲得件數</td><td>0</td><td>0</td><td>100%</td><td></td></tr>
<tr><td rowspan="2">技術移轉</td><td>件數</td><td>0</td><td>0</td><td>100%</td><td>件</td><td></td></tr>
<tr><td>權利金</td><td>0</td><td>0</td><td>100%</td><td>千元</td><td></td></tr>
<tr><td rowspan="4">參與計畫人力（外國籍）</td><td>碩士生</td><td>0</td><td>0</td><td>100%</td><td rowspan="4">人次</td><td></td></tr>
<tr><td>博士生</td><td>0</td><td>0</td><td>100%</td><td></td></tr>
<tr><td>博士後研究員</td><td>0</td><td>0</td><td>100%</td><td></td></tr>
<tr><td>專任助理</td><td>0</td><td>0</td><td>100%</td><td></td></tr>
</table>

	成果項目	量化	名稱或內容性質簡述
其他成果 (無法以量化表達之成果如辦理學術活動、獲得獎項、重要國際合作、研究成果國際影響力及其他協助產業技術發展之具體效益事項等,請以文字敘述填列。)	本研究成果將有潛力成為高引用論文。		

	成果項目	量化	名稱或內容性質簡述
科教處計畫加填項目	測驗工具(含質性與量性)	0	
	課程/模組	0	
	電腦及網路系統或工具	0	
	教材	0	
	舉辦之活動/競賽	0	
	研討會/工作坊	0	
	電子報、網站	0	
	計畫成果推廣之參與(閱聽)人數	0	

國科會補助專題研究計畫成果報告自評表

請就研究內容與原計畫相符程度、達成預期目標情況、研究成果之學術或應用價值（簡要敘述成果所代表之意義、價值、影響或進一步發展之可能性）、是否適合在學術期刊發表或申請專利、主要發現或其他有關價值等，作一綜合評估。

---

1. 請就研究內容與原計畫相符程度、達成預期目標情況作一綜合評估

   ■達成目標

   □未達成目標（請說明，以 100 字為限）

   　　　□實驗失敗

   　　　□因故實驗中斷

   　　　□其他原因

   　說明：

---

2. 研究成果在學術期刊發表或申請專利等情形：

   論文：■已發表 □未發表之文稿 □撰寫中 □無

   專利：□已獲得 □申請中 ■無

   技轉：□已技轉 □洽談中 ■無

   其他：（以 100 字為限）

   目前相關成果除了已發表之論文乙篇(如精簡報告中所列)外，尚有其它相關論文仍在撰寫中。

---

3. 請依學術成就、技術創新、社會影響等方面，評估研究成果之學術或應用價值（簡要敘述成果所代表之意義、價值、影響或進一步發展之可能性）（以 500 字為限）

   本研究成果首次以實驗數據，清楚展現出奈米結構能有效提昇薄膜型熱電材料之特性，對於未來之產業應用或是學術研究均為重要之參考資料。